ELSEVIER

Fusion Engineering and Design 32–33 (1996) 267–275

Fusion Engineering and Design

Intense heavy ion beam transport with electric and magnetic quadrupoles

T.J. Fessenden[a], J.J. Barnard[b], M.D. Cable[b], F.J. Deadrick[b], M.B. Nelson[b], T.C. Sangster[b], S. Eylon[a,1], H.S. Hopkins[c]

[a]*Lawrence Berkeley National Laboratory, Berkeley, CA, USA*
[b]*Lawrence Livermore National Laboratory, Livermore, CA, USA*
[c]*University of California at Berkeley, Berkeley, CA, USA*

Abstract

As part of the small induction recirculator development at LLNL we are testing an injector and transport line that delivers 4 μs beams of potassium with repetition rates up to 10 Hz at a nominal current of 2 mA. The normalized edge equivalent emittance of the beams is near 0.02 mm mrad and is mostly determined by the temperature of the source (0.1 eV). K^+ ions generated at 80 keV in a Pierce diode are matched to an alternating gradient transport line by seven electric quadrupoles. Two additional quads have been modified to serve as two-axis steerers. The matching section is followed by a transport section comprised of seven permanent magnet quadrupoles. Matching to this section is achieved by adjusting the voltages on the electric quadrupoles to voltages calculated by an envelope matching code. Measurements of beam envelope parameters are made at the matching section entrance and exit as well as at the end of the permanent magnet transport section. Beam current waveforms along the experiment are compared with results from a one-dimensional longitudinal dynamics code.

Initial experiments show particle loss occurring at the beam head as a result of overtaking. Except for this, the beam is transported with essentially no loss of current through the 4.8 m of electric and magnetic focused transport. During transport the emittance increases by approximately 50% from the intrinsic emittance of the source. Some electron effects that have little apparent influence on transport have also been seen.

The apparatus is also being used for the development of non- or minimally intercepting diagnostics for future recirculator experiments. These include capacitive monitors for determining beam line change density and position in the recirculator, flying wire scanners for beam position, and gated TV scanners for measuring beam profiles and emittance.

1. Introduction

Lawrence Livermore National Laboratory (LLNL), in collaboration with Lawrence Berkeley National Laboratory (LBNL) and EG&G, is building a small recirculating induction accelerator of singly charged potassium ions to investigate the fundamental physics and engineering issues of this novel accelerator concept. The small recirculator is designed to accelerate K^+ ion beams with an initial energy of 80 keV, a current of 2 mA, pulse duration 4 μs and repetition rate up to 10

[1] Participating guest.

PII S0920-3796(96)00478-4

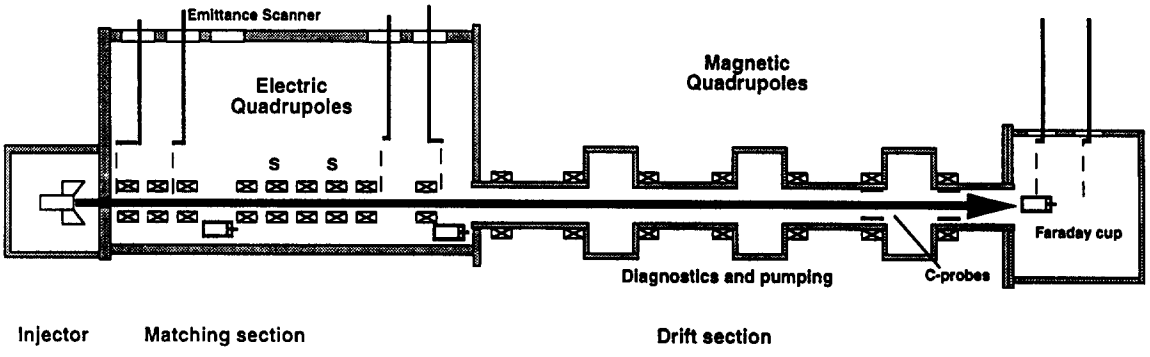

Fig. 1. Diagram of potassium ion beam transport apparatus. The length from injector to final Faraday cup is 4.86 m.

Hz at a normalized emittance of less than 0.1 mm mrad. This paper describes progress toward the completion of the injector system that will provide the initial beam for injection into the small recirculator. We describe the apparatus, the characterization of the potassium beams generated by the injector, the transport of beams through the electric focused matching system and the magnetic focus beam transport system, and the status of diagnostic system development.

We are also interested in the transport of space-charge-dominated ion beams with a magnetic quadrupole transport system. This method of beam transport is planned for over 90% of the total length for almost all heavy ion fusion (HIF) accelerator–driver concepts under study. Magnetic quadrupole transport of intense ion beams was the subject of an experimental study [1] at GSI (Gesellschaft für Schwerionenforschung) in Darmstadt, Germany. In those experiments, spurious electrons partially neutralized the ion beam and affected beam transport. HIF accelerator physics experiments at LBNL have almost exclusively used electric quadrupoles for beam transport. In these experiments the strong transverse electric fields of the quadrupoles quickly removed spurious electrons.

2. Experimental description

The potassium ion beam is obtained from a contact ionization source in the diode injector [2] shown in Figs. 1 and 2. The source is mounted on a Pierce shaped graphite anode plate connected to an 80 kV pulser. The source uses a porous tungsten surface 2.54 cm diameter which is coated with a layer of aluminosilicate (zeolite). Potassium ions are emitted by surface ionization when the source is heated to about 980 °C. The heater power (about 150 W) is delivered through a high voltage isolation transformer. The anode pulser consists of a switched pulse forming line that operates near 20 kV. A step-up transformer increases this voltage to 80 kV. The resulting pulse waveform can be seen in Fig. 3. The current of the beam injected into the matching system is controlled by the diameter (1.04 cm) of the injector output aperture. The intrinsic normalized emittance ε_n of the source, as determined by the source temperature, is approximately 0.02 mm mrad.

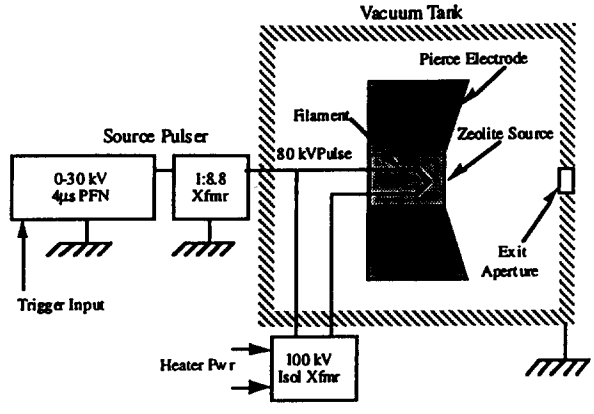

Fig. 2. Diagram of K^+ ion injector system.

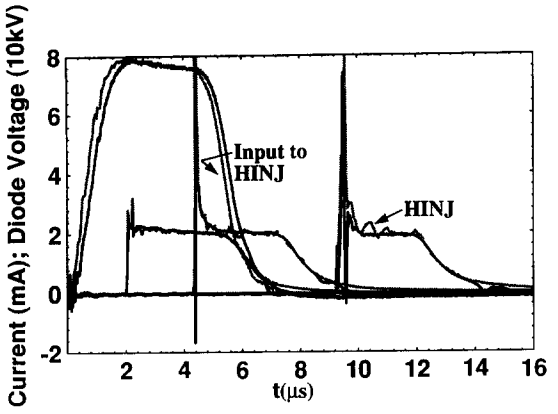

Fig. 3. Measured (dark) and corrected (gray) voltage monitor waveforms and measured (dark) and HINJ (gray) current waveforms at three positions along experiment. The negative spike at position two is caused by a spurious response that often occurs when the beam is bigger than the Faraday cup. The HINJ current waveforms appear noisier than the experimental waveforms because of the numerical derivatives required to calculate V_{diode}.

The matching system consists of seven electric quadrupoles. The first three are 15.24 cm (6 in) apart and the last seven are 30.48 cm (12 in) apart. Between the fourth and fifth and the fifth and sixth quadrupoles are two-axis steering dipoles for centering and aligning the beam on to the axis. These are marked with an "s" in the diagram of the experiment shown in Fig. 1.

Following the matching section is a drift section that uses seven samarium–cobalt permanent magnet quadrupoles to transport the beam to a diagnostic box. The quadrupoles have a focus strength ($\int B' \, dz$) of 0.93 T, are 10 cm long and have a peak field of 0.3 T at a radius of 3.5 cm. They are located 38.1 cm (15 in) apart. Three locations in the drift section are available for diagnostics and pumping.

For these experiments the matching section and transport sections were pumped by a single 20 in cryopump located in the top plate of the matching section. The injector was pumped by a 10 in cryopump. Typical pressures in the injector are $(3–5) \times 10^{-7}$ Torr, in the matching section $(4–5) \times 10^{-8}$ Torr and at the end of the drift section 6×10^{-7} Torr.

Diagnostics for the experiment include insertable double-slit emittance scanners and Faraday cups located as shown in Fig. 1. Capacitive monitors that measure the beam line charge density and mean position were located under the sixth and seventh magnetic quadrupoles. These are discussed in Section 6. At one time an electrostatic beam energy analyzer, developed at LBNL, was located between quads 8 and 9 in the matching section. Fig. 4 contains measurements of beam energy obtained with the analyzer.

3. Beam current evolution

The beam current is determined by the voltage pulse applied to the injector and therefore varies approximately as the 3/2 power of the injector voltage. Thus both the beam current and energy evolve with time. The space charge of the beam also causes it to elongate as it drifts through the apparatus. We use Faraday cup measurements, an energy analyzer and a 1D longitudinal dynamics code (HINJ) [3] to obtain a quantitative understanding of this longitudinal beam evolution.

The beam current is measured with Faraday cups near the beginning (0.67 m) and end (1.7 m) of the electric matching section and at the end of the magnetic transport (4.86 m) section as shown in Fig. 1. The electrostatic energy analyzer was located 1.6 m downstream of the source. The drift distance to the detector of the analyzer was 1.75 m. Fig. 3 shows measurements of the beam cur-

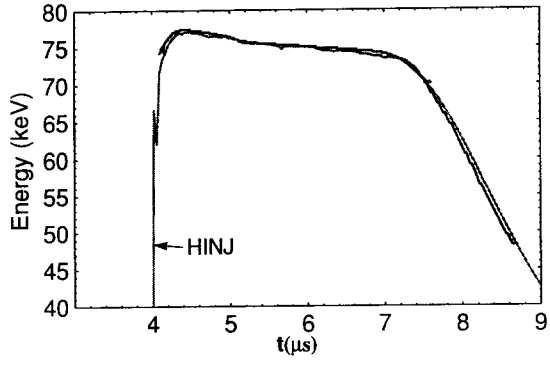

Fig. 4. Energy analyzer measurements (dark) and HINJ predictions (gray). The calibration constant α was adjusted to produce the best match of the HINJ prediction with the experimental data.

rent at the three Faraday cup locations. Also plotted are results from the 1D code HINJ showing close agreement between simulation and experiment. The large current spike at the head of the pulse is caused by particle overtaking occurring at the beam head. The exponential rise time of the diode voltage waveform is nearly 1 μs, which is longer than the ideal rise time of about 0.36 μs [4]. With the slower rise time, ions emitted at the beginning of the pulse travel slower than ions emitted subsequently and so particle overtaking occurs, generating the current spike. The beam size tends to vary as the square root of the current. As a consequence the beam head is constantly eroding as the beam travels along the experiment.

The HINJ code uses the actual voltage waveform that appears across the diode to begin its calculations. A measurement of the step response of the voltage monitor circuit showed that the voltage monitor has a rise time τ of approximately 0.2 μs. To obtain good agreement between the code and the experiment, it was necessary to correct for this rise time. From the measurement the impulse response of the voltage monitor circuit is approximated by an exponential with a fall time of 0.2 μs divided by a calibration constant α. Since the detected output is a convolution of the actual diode voltage and the impulse response of the voltage monitor, the diode voltage is given in terms of the monitored voltage by

$$\alpha V_{\text{diode}}(t) = V_{\text{monitor}} + \tau \frac{\mathrm{d}V_{\text{monitor}}}{\mathrm{d}t} \qquad (1)$$

The measured monitor voltage was digitized and corrected using Eq. (1) for use by the HINJ code. Both the measured and corrected waveforms are shown in Fig. 3. In practice the derivative contributes numerical noise to the corrected diode voltage waveform.

The calibration of the high voltage monitor was checked by three independent methods. The first compared the monitor voltage with a high voltage Tektronix probe at reduced voltage. The second was to determine the beam energy vs. time with the electrostatic energy analyzer and compare with the HINJ code results. Because of fringe fields at the input and exit of the analyzer, the absolute accuracy of this method is limited to approximately $\pm$ 5%. The third and perhaps most accurate method was to adjust the calibration constant α until the current waveforms at the known positions of the Faraday cups match up with corresponding current waveforms from HINJ. Changes as small as 1% could easily be detected. This method essentially constitutes a time-of-flight measurement through a drift section nearly 5 m long. The three independent measurements yielded results within 5%.

4. Beam matching and transport

The beam at the output of the injector is round and diverging at an angle of 18 mrad and must be matched to the transport system. The electric matching section was originally used with the Single Beam Transport Experiment (SBTE) [5] at LBNL. The injector was designed with an output grid to produce a parallel beam at the exit. However, heat from the source distorted the grid, resulting in a very non-uniform beam. Removing the grid improved the uniformity but added a diverging electrostatic exit lens which produces the diverging beam. A double-slit scanner visible in Fig. 1 is used to determine the Y beam envelope parameters at the input to the matching section. As no X-oriented scanner was available, the X envelope parameters were assumed to equal the Y parameters. These parameters are input to an electrostatic envelope code MATCH that is used to calculate the quadrupole focus voltages for the electric matching section. This code uses a hard edge linear model for the electric quadrupoles. By varying four quadrupole voltages, the code finds the voltages that produce the four requested X and Y envelope parameters (x, $\mathrm{d}x/\mathrm{d}z$, y, $\mathrm{d}y/\mathrm{d}z$) at a downstream location. For this experiment we chose the location to be the input to the magnetic transport section and the requested envelope parameters to be those that match the beam to this section. Fig. 5 shows envelopes of the beam in the two sections of the experiment. Note that the beam is somewhat mismatched in the electric section in order to achieve a match in the magnetic section.

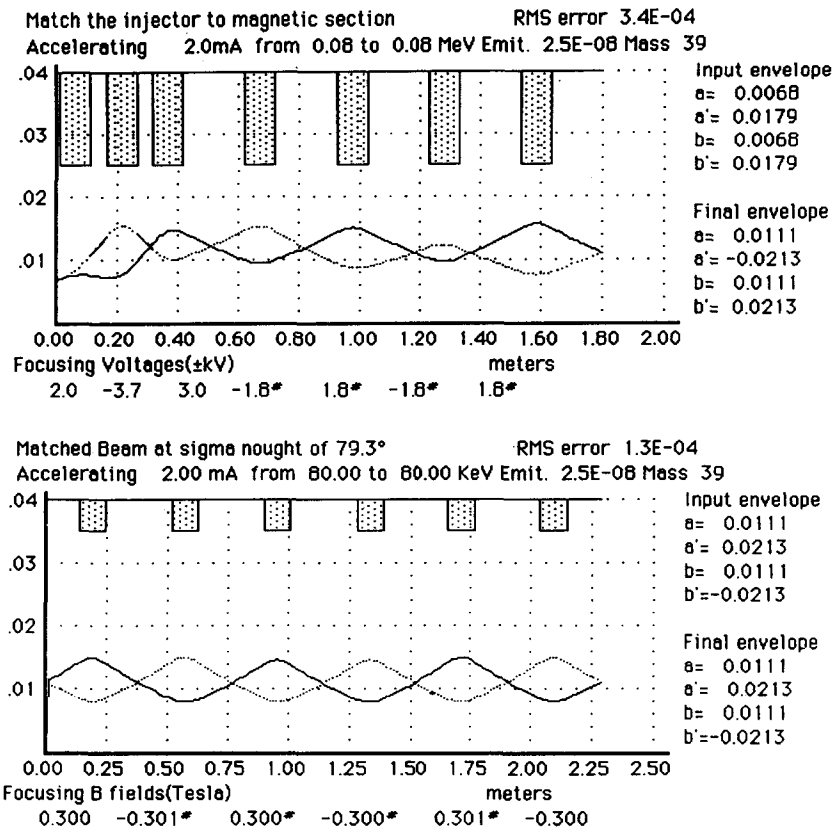

Fig. 5. Beam envelopes in electric matching and magnetic transport sections. The electric quadrupoles in the matching section are adjusted to match the round beam from the injector to the permanent magnet quadrupole transport section. For these parameters the depressed phase advance in the magnetic transport section is approximately 7.5°.

The magnetic transport section consists of seven permanent magnet quadrupoles that form a transport lattice with period 76.2 cm (30 in). The undepressed phase advance per period for K^+ at 80 keV in this lattice is 79.3°. At a normalized edge emittance of 0.04 mm mrad the depressed phase advance per period is 7.5°. We encountered no difficulties (aside from an initially rotated quad) in transporting beams 2.8 m at pressures below 10^{-5} Torr using permanent magnet quadrupoles. Except for the loss due to overtaking at the beam head which persisted through the magnetic transport section, no detectable current loss over the body of the pulse was observed. Some evidence of electrons was detected with the capacitive monitors as described in Section 6. These had little influence on transport at pressures below 10^{-5} Torr.

5. Beam emittance measurements

The beam emittance is measured at three z locations using the double-slit scanning techniques [5] as implemented at LBNL. An upstream slit is scanned across the beam to produce a fan beam 0.1 mm wide that is allowed to spread owing to its internal transverse energy. A second movable 0.1 mm slit–Faraday cup approximately 250 mm downstream measures the beam spreading. Together these are converted into a K–V emittance according to the relation

$$\varepsilon_n = 4\beta\varepsilon_{rms}$$

$$= 4\beta(\langle\chi\rangle^2\langle\theta\rangle^2 - \langle\chi\theta\rangle^2) \quad \text{(mm mrad)} \qquad (2)$$

Here χ is the weighted beam position and θ is the angle from the axis as determined by the relative position of the two slits. For the calculation, 90%

Table 1
Measurements of beam parameters at three scanner locations together with parameters calculated by MATCH code

Location	Z (m)	ε_n (90%) (mm mrad)	$2x_{rms}$ (mm)	x_{code} (mm)	$2\theta_{rms}$ (mrad)	θ_{code} (mrad)
Source exit	0.09	0.025	6.8 (input)	6.8	18.0	18.0 (input)
Matching exit	1.74	0.030	12.7	11.1	18.9	21.3
End of exp. (y)	4.75	0.039	12.0	17.5	15.7	29.5
End of exp. (x)	4.75	0.042	3.6	6.8	−17.7	−13.6

of the particles are used. The information is also processed to generate the beam envelope parameters at the location of the scanner.

Table 1 contains the results of measurements of envelope parameters at the three accessible locations along the experiment. The scanner at the end of the machine was rotated by 90° to obtain a measurement in the x direction. The envelope parameters calculated by the MATCH code are presented for comparison. These results suggest that the actual beam envelope in the magnetic transport section is not as well matched as suggested by Fig. 5 and that more frequent measurements of the beam envelope will be required to ensure the match. Additional beam scanners are being fabricated for insertion in the diagnostic access points in the matching section. The measurements also show that the beam emittance increases by approximately 0.015 mm mrad as the beam drifts through the apparatus. This small increase could result from any number of causes, including beam mismatch, electron effects, transport at highly depressed tune, focus non-linearities, etc. Experimentally, small changes in emittance stand out because the emittance is so low to start with. None the less, the cause of the emittance increase is of considerable interest and will be the subject of study in future experiments and simulations.

6. Capacitive monitors, operation and results

For successful operation of the recirculator the position of the beam must be known and accurately controlled over each revolution of the beam. We are currently developing [6] simple

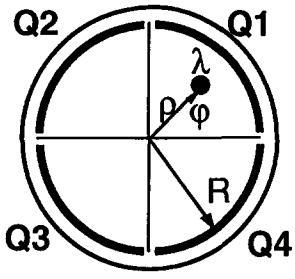

Fig. 6. Sketch of capacitive monitor geometry.

capacitive beam intensity and position monitors that will be placed under each permanent magnet quadrupole of the recirculator. The basic design of the monitor consists of four sensor segments as illustrated in Fig. 6. An unneutralized beam will induce a total charge on the four sectors Q_1, Q_2, Q_3 and Q_4 of λL, where λ is the beam line charge density and L is the length of the monitors. Only if the beam centroid coincides with the axis will these four charges be equal. By measuring these charges vs. time, the beam intensity and position in the pipe can be determined.

An analytic expression for the charge induced on sector Q_1 is given by

$$\frac{Q_1}{L} = \frac{\lambda}{2\pi} \int_0^{\pi/2} \frac{1-\rho^2}{1+\rho^2-2\rho\cos(\vartheta-\varphi)} \, d\vartheta \qquad (3)$$

for a beam of intensity λ that is off axis by an amount ρ at an angle φ. Similar expressions exist for the other three sectors.

By adding and subtracting the charges on the respective plates, one finds the following relations between the induced charges and the beam offsets:[2]

[2] We thank D.L. Judd (LBNL) for pointing out that Eqs. (4) and (5) could be written in this simplified form.

$$\frac{Q_1+Q_4-Q_2-Q_3}{Q_1+Q_2+Q_3+Q_4}=\frac{2}{\pi}\tan^{-1}\left(\frac{2\rho\cos\varphi}{1-\rho^2}\right)\approx\frac{4x}{\pi R} \tag{4}$$

$$\frac{Q_1+Q_2-Q_3-Q_4}{Q_1+Q_2+Q_3+Q_4}=\frac{2}{\pi}\tan^{-1}\left(\frac{2\rho\sin\varphi}{1-\rho^2}\right)\approx\frac{4y}{\pi R} \tag{5}$$

Here x and y are the beam displacements and R is the radius of the monitor. For radial displacements less than $R/2$ the approximations produce an error less than 7%. If the beam velocity at the position of the monitor is known, the beam current can be found from

$$I_{\text{beam}}=\frac{v(Q_1+Q_2+Q_3+Q_4)}{L} \tag{6}$$

The charge on each of the four sectors is found by measuring the voltage induced on the capacitor formed by each plate to ground plus any external capacitance used in sensor cabling. Errors in the determination of these capacitances will contribute to errors in determining the beam intensity; relative errors appear as errors in determining beam offsets. The signal voltage is inversely proportional to the total system capacitance and thus it is desirable to keep the cable length as short as possible or to locate high impedance buffer amplifiers in the vicinity of the monitor. Signals are acquired by two LeCroy 6840 CAMAC dual transient digitizer modules and the beam position is calculated with a Macintosh computer.

Fig. 7a shows initial measured waveforms on each of the sectors of a C-monitor located under the seventh magnet of the transport section. Note that the waveforms are good replicas of the beam current waveform, but that the magnitudes of the four are not equal, implying that the beam is off axis. Fig. 7b shows the beam position vs. time as resolved from these signals assuming equal channel gains. As yet we have not had an opportunity to perform an experiment that independently measures the beam position for comparison with the C-monitor determination. Also shown in Fig. 7b is the result of "centering" the beam at the position of the monitor by using the steering dipoles in the electric matching section.

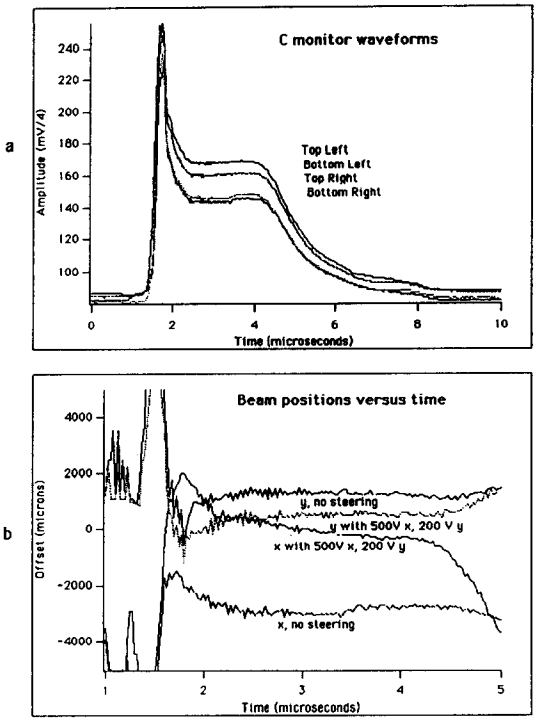

Fig. 7. Oscillograms obtained from capacitive charge monitor. Fig. 7a shows the voltages detected on each of the four sectors of the monitor. Fig. 7b shows the reduction of these signal using the approximate forms of Eqs. (4) and (5). Also shown is the result of steering the beams to the electrical axis using the electric steering dipoles in the matching section.

These monitors are very sensitive to stray electrons. At gas pressures greater than approximately 10^{-5} Torr we found that spurious electrons generate voltages at the end of the pulse comparable with the signal. Adding a d.c. bias voltage of -50 V to each of the plates rejected these unwanted electrons. At pressures below 10^{-6} Torr no bias voltages were required.

By biasing the electrodes to voltages comparable with the beam space charge potential (amount 100 V), some electrons could be detected at the time the ion beam was present. The experiment suggested a more or less constant electron current that was approximately 100 times more than the current one might expect from direct beam ionization of the residual gas in the immediate vicinity of the monitor. We do not as yet have a satisfactory explanation of these results, but we plan to investigate further.

7. Other diagnostics under development

7.1. Gated beam imager

In order to make rapid measurements of the beam shape and emittance, a gated beam imaging system is being developed. The diagnostic will consist of a sheet of fast plastic scintillator (Bicron Corp. BC-412) that intercepts the beam and is imaged by a CCD camera with a gated image intensifier. The spatial dependence of the beam intensity in a "slice" of the beam in the $x-y$ plane can then be obtained by gating the camera system on for some length of time (currently planned to be 50 ns) at the appropriate time during the beam pulse. Multiple pulses can be used to vary the position of this slice longitudinally along the beam pulse, thus obtaining a complete 4D (x, y, z and intensity) beam mapping. A plate with small holes upstream from the diagnostic can be introduced and gated images of the resulting spots used to determine the transverse velocity of the beam at the various sample points. Again, multiple pulses can be used to give an emittance measurement over the entire beam.

We are addressing concerns about possible damage to the scintillator caused by the ion beam. Initial experiments with a non-imaging photomultiplier tube showed no degradation (bleaching) of the scintillator light output after repeated exposure to the ion beam. Moreover, measurements of the output light vs. time reproduced the Faraday cup signals. However, initial experiments with a TV camara to image the scintillator light are showing some evidence of image degradation. These experiments are continuing.

7.2. Rotating wire scanner

Since multilap operation of the recirculator will preclude the use of intercepting diagnostics, we are developing a quasi-non-intercepting rotating wire scanner to measure the beam shape and position. Although stringent space requirements on the half-lattice periods of the recirculator will probably require the development of a custom device, initial tests of the scanner are being done with a commercially available instrument, the National Electrostatics Corp. Beam Profile Monitor Model BPM82. The device consists of a single wire formed into a 45° helix that is rotated about the axis of the helix. The wire sweeps across the center of the beam in two orthogonal directions with every revolution. Appropriate triggering of the beam pulse will allow it to intercept the wire at various positions. The signal from the wire is recorded by a 40 megasample per second transient digitizer, resulting in a current vs. z measurement for a 1 mm slice (the wire diameter) across the beam. Multiple beam pulses can be used to build up an entire beam profile. Initial tests of the unmodified commercial system, which uses a grounded wire surrounded by an isolated housing intended to collect scattered electrons, showed an undesirable amount of capacitive pickup from the beam space charge. The mechanical configuration is being modified to eliminate the housing, isolate the wire and directly monitor electrons emitted from the wire by ion impacts.

8. Final comments and conclusions

This paper reports work in progress on the development of a suitable injector for the induction recirculator experiment. These initial results are encouraging in that, except for the pulse head, the very cold potassium beam is transported over the 4.8 m of the experiment by the electric and magnetic quadrupoles with minimal emittance growth.

The envelope code prediction of the envelope parameters is in reasonable agreement with the experimental results from the emittance scanners. However, the agreement between the two in the magnetic transport section is not as good. More frequent measurements of the beam envelope and/or improvements in the code model of the experiment may be required. It is also possible that the lack of agreement results from the effects of spurious electrons on the beam envelope. More experiments are required to elucidate this issue.

A major shortcoming of the present system is the 1 μs rise time of the diode pulser that drives the injector diode. Because of its slow rise time, particle overtaking occurs and the pulse head

erodes over the entire length of the experiment. A new pulser with a rise time of approximately 0.3 μs is nearly complete. This pulser should improve the longitudinal match to the transport channel and greatly reduce the overtaking and particle loss at the beam head.

Most likely because of our much shorter pulse duration, we observe no significant effects caused by beam neutralization as did Klabunde et al. [1]. Using estimates of the ionization cross-section even as high as 10^{-15} cm^2 for K^+ against the background gas, we conclude that our 4 μs beam should be less than 1% neutralized at 10^{-6} Torr. As the beam duration is increased or the beam is recirculated in a storage ring or accelerator, beam neutralization can be expected to become more of an issue and will need to be controlled by improving the vacuum pumping.

Acknowledgements

We are pleased to acknowledge the many helpful discussions with our colleagues in the heavy ion fusion groups at LLNL led by Alex Friedman and at LBNL led by Roger Bangerter. We also wish to acknowledge the engineering support provided by Dave Longinotti, Chuck Ward and John Meredith of EG&G and by Larry Nattress and colleagues at LLNL as well as the technical support of Geoff Mant and Dave Pendleton.

This work was performed under the auspices of the US DoE by LLNL and LBL under contracts W-7405-ENG-48 and DE-AC03-76SF00098.

References

[1] J. Klabunde, M. Reiser, A. Schoenlein, P. Spadtke and J. Struckmeier, Studies of heavy ion beam transport in a magnetic quadrupole channel, IEEE Trans. Nucl. Sci. NS-30(4) (1983), p. 2543.

[2] S. Eylon, E. Henestroza and F. Deadrick, K^+ diode for the LLNL heavy ion recirculator accelerator experiment, Proc. Particle Accelerator Conf., Dallas, TX, May 1995, IEEE, Piscataway, NJ, 1996, p. 905.

[3] J.J. Barnard, G.C. Caporaso, S.S. Yu and S. Eylon, 1-D simulations of heavy-ion injectors, Proc. Particle Accelerator Conf. Washington, DC, May 1993, Vol. 1, IEEE, Piscataway, NJ, 1993, p. 712.

[4] M. Lampel and M. Tiefenback, An applied voltage to eliminate current transients in a one-dimensional diode, Appl. Phys. Lett. 43 (1983) 57.

[5] M.G. Tiefenback, Space-charge limits on the transport of ion beams in a long alternating gradient system, LBL-22465, 1986, p. 38.

[6] F.J. Deadrick, J.J. Barnard, T.J. Fessenden, J.W. Meridith and J. Rintamaki, Development of beam position monitors for heavy ion recirculators, Proc. Particle Accelerator Conf., Dallas, TX, May 1995, IEEE, Piscataway, NJ, 1996, p. 2557.